

Fig. 3. Effects of pitavastatin on sirolimus-induced down regulation of eNOS and Akt (a representative down stream signal of eNOS) in human aortic endothelial cells. Pitavastatin normalized sirolimus-induced decrease in phosphorylated (activated) eNOS and Akt. Data are the mean \pm SEM ($n=6$ each). $p < 0.05$ or 0.01 versus no treatment by one-way ANOVA followed with Dunnett's multiple comparison test.

(Table 2). Thus, the angiographically examined in-stent stenosis was less in the pitavastatin-NP group than in the control and FITC-NP groups. The sirolimus-eluting stent showed similar inhibitory effects on markers of in-stent stenosis.

Histological analysis demonstrated that a significant in-stent neointima formed similarly at the bare metal stent and FITC-NP-eluting stent sites (Fig. 5). Quantitative analysis demonstrated that pitavastatin-NP-eluting stents attenuated in-stent neointima formation as effectively as sirolimus-eluting stents.

Effects of Pitavastatin-NP-Eluting Stents Versus Sirolimus-Eluting Stents on Inflammation and Fibrin Deposition

Micrographs of coronary artery cross-sections stained with hematoxylin-eosin from FITC-NP-eluting, pitavastatin-NP-eluting, and sirolimus-eluting stent groups are shown in Fig. 6. A semi-quantitative histological scoring system demonstrated that there was no significant difference in the injury score among the four groups four weeks after stenting (Table 3).

Inflammatory cells consisting mainly of macrophages were recruited around the stent wire and into the neointimal layer in all four sites; however, the inflammation score was significantly less at the pitavastatin-NP-eluting stent site than in the bare metal stent site (Table 3). At the sirolimus-eluting stent site, the inflammation score was greater than at the bare metal stent and pitavastatin-NP-eluting stent

FBS-induced proliferation of human coronary artery SMCs (cell number/well)

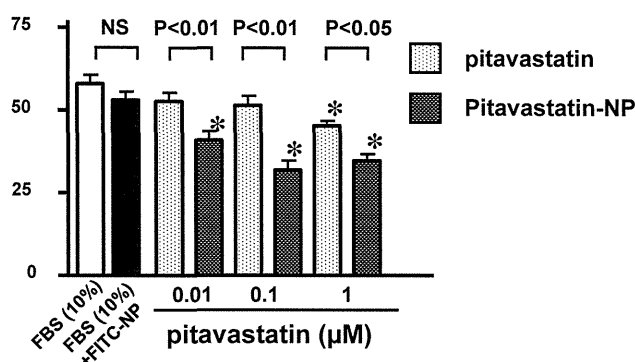


Fig. 4. Effects of pitavastatin and pitavastatin-NP on the FBS-induced proliferation of human CSMCs. Data are the mean \pm SEM ($n=6$ each). $*p < 0.01$ versus no treatment by one-way ANOVA followed with Dunnett's multiple comparison test.

sites (Table 3).

Minor fibrin deposition was observed at bare metal, FITC-NP-eluting, and pitavastatin-NP-eluting stent sites (Table 3). At the sirolimus-eluting stent site, the fibrin score was significantly higher than at the bare metal stent site, and this difference was even more significant when compared with the pitavastatin-NP-eluting stent site.

To determine whether the therapeutic effects of

Table 2. Coronary angiographic parameters (coronary artery diameter, in-stent stenosis) before, immediately after, and 4 weeks after stent implantation in porcine coronary artery

	BMS (n=10)	FITC-NP stent (n=12)	Pitavastatin -NP stent (n=12)	SES (n=12)	<i>p</i> value
Coronary diameter before stent implantation	2.19 ± 0.04	2.25 ± 0.05	2.41 ± 0.06	2.42 ± 0.10	NS
Coronary diameter immediately after stent implantation	2.70 ± 0.06	2.75 ± 0.05	2.79 ± 0.03	2.89 ± 0.04	NS
Stent-to-artery ratio immediately after stent implantation	1.20 ± 0.02	1.22 ± 0.03	1.13 ± 0.02	1.19 ± 0.04	NS
Coronary diameter 4 weeks after stent implantation	1.45 ± 0.13	1.51 ± 0.10	2.02 ± 0.12*	2.02 ± 0.15*	0.0025
Angiographically-examined in-stent restenosis 4 weeks after stent implantation (% diameter stenosis)	42.9 ± 4.9	46.0 ± 3.4	25.8 ± 3.5*	27.2 ± 3.7*	0.0003

Data are the mean ± SEM. NS=not significant

**p* < 0.05 versus control bare metal stent by Bonferroni's multiple comparison tests

the pitavastatin-NP-eluting stent are mediated by local or systemic mechanisms, effects of intracoronary administration of pitavastatin-NP on histopathological features after deployment of bare metal stents were examined (Table 4). Pitavastatin-NP at 300 µg showed no therapeutic effects on indices of in-stent stenosis and adverse effects on histopathological scoring. Pitavastatin-NP at 3000 µg also had no effects on indices of in-stent stenosis, but modestly but significantly decreased fibrin deposition.

Effects of Pitavastatin-NP-Eluting Stents Versus Sirolimus-Eluting Stents on Endothelial Surface Coverage

As previously reported, re-endothelialization was not impaired at sirolimus-eluting stent sites four weeks post-stenting. There was no significant difference in the re-endothelialization score among the four groups four weeks after stenting (Table 3); therefore, the endothelial surface coverage was examined at earlier time points (seven days post-stenting) by scanning electron microscopy. At bare metal stent sites, almost complete endothelial coverage was noted above and between stent struts at seven days (Fig. 7). Similar magnitudes of endothelial coverage were observed at FITC-NP-eluting stent and pitavastatin-NP-eluting stent sites. In contrast, endothelial coverage was impaired at sirolimus-eluting stent sites; regions lacking endothelial coverage were generally associated with platelet aggregation and adherent leukocytes.

Serum and Tissue Concentrations of Pitavastatin

Tissue concentrations of pitavastatin were below the limit of detection (2.5 ng/g protein) in coronary artery segments three hours after the deployment of pitavastatin-NP-eluting stents. In addition, serum levels of pitavastatin were below the limit of detection (1 ng/mL) one and three hours after the deployment of pitavastatin-NP-eluting stents.

Discussion

We here report the first successful development of pitavastatin-NP-eluting stents with a newly invented cationic electrodeposition coating technology. We previously showed that (1) PLGA-NP was taken up actively by VSMC and endothelial cells mainly via endocytosis and was retained stably in the intracellular space and that (2) NPs may slowly release encapsulated drugs as PLGA is hydrolyzed^{22, 23}. This bioabsorbable polymeric NP-eluting stent system has unique aspects with respect to vascular compatibility and efficient drug delivery (stable delivery of NPs into the neointima and medial layers until day 28 after deployment of the NP-eluting stent), as compared to dip-coated polymer-eluting stents²². Importantly, this NP drug delivery system can carry hydrophilic agents such as statins, which offer advantages over the current stent-coating technology. In addition, this NP-eluting stent system provided an effective means of delivering NP-incorporated drugs or genes that target intracellular proteins involved in the pathogenesis of

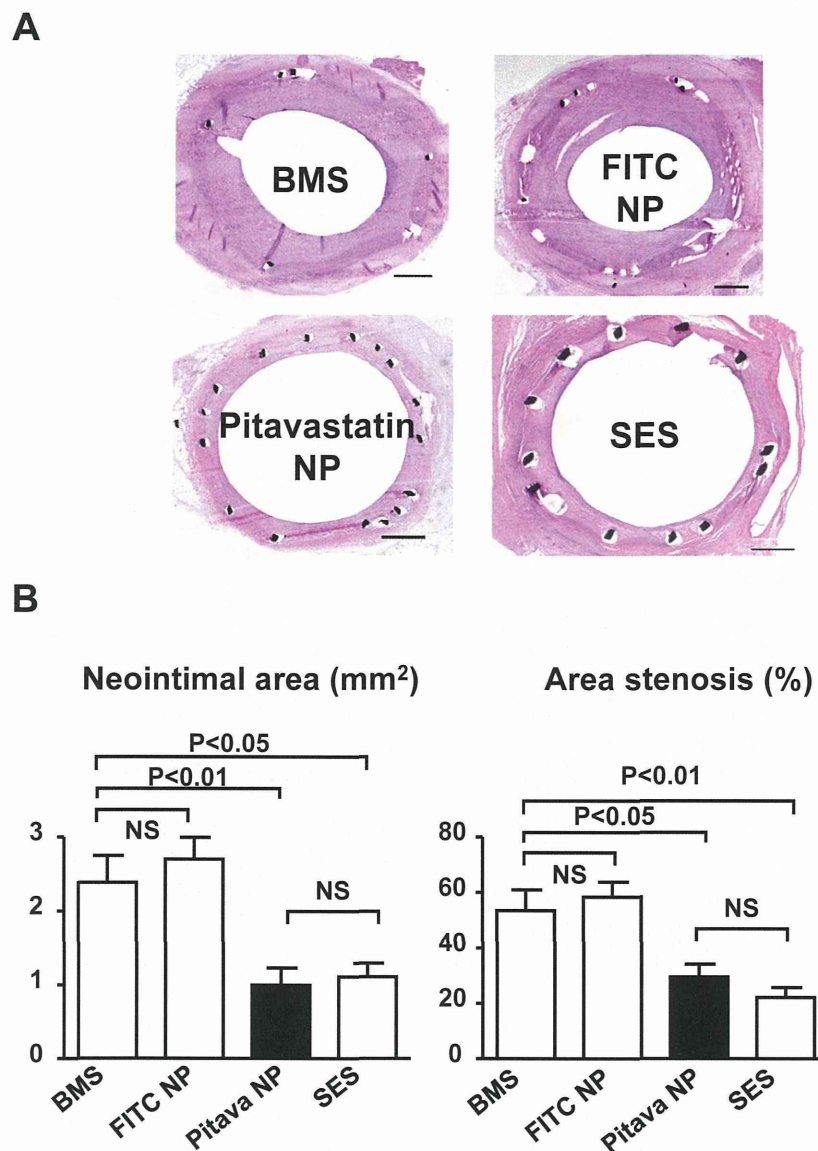


Fig. 5. Histopathological analysis of in-stent neointima formation four weeks after stent implantation.

A, Coronary artery cross-sections stained with hematoxylin-eosin from bare metal stent (BMS), FITC-NP-eluting, pitavastatin-NP-eluting, and sirolimus-eluting stent (SES) groups. Bar=0.5 mm. B, Neointima area (mm²) and % stenosis [$100 \times (\text{area of internal elastic lamia} - \text{neointima area}) / \text{area of internal elastic lamia}$] in bare metal stent ($n=10$), FITC-NP-eluting stent ($n=12$), pitavastatin-NP-eluting stent ($n=12$) stent, and sirolimus-eluting stent ($n=12$) groups.

in-stent neointima formation; therefore, this NP-eluting stent system may work as an excellent platform for delivering therapeutic agents.

The pleiotropic (non-LDL-related) vasculoprotective effects of statins are mediated through reduced levels of cholesterol biosynthesis intermediates that serve as lipid attachments for posttranslational modifi-

cations (isoprenylation) of proteins, including Rho and Rac⁸). In the present study, pitavastatin was selected as the nanoparticulation compound because this compound elicited (1) the most potent inhibitory effects on human VSMC proliferation (**Table 1**), and (2) the greatest effects on the re-endothelialization response of human endothelial cells and on the inhibition of tis-

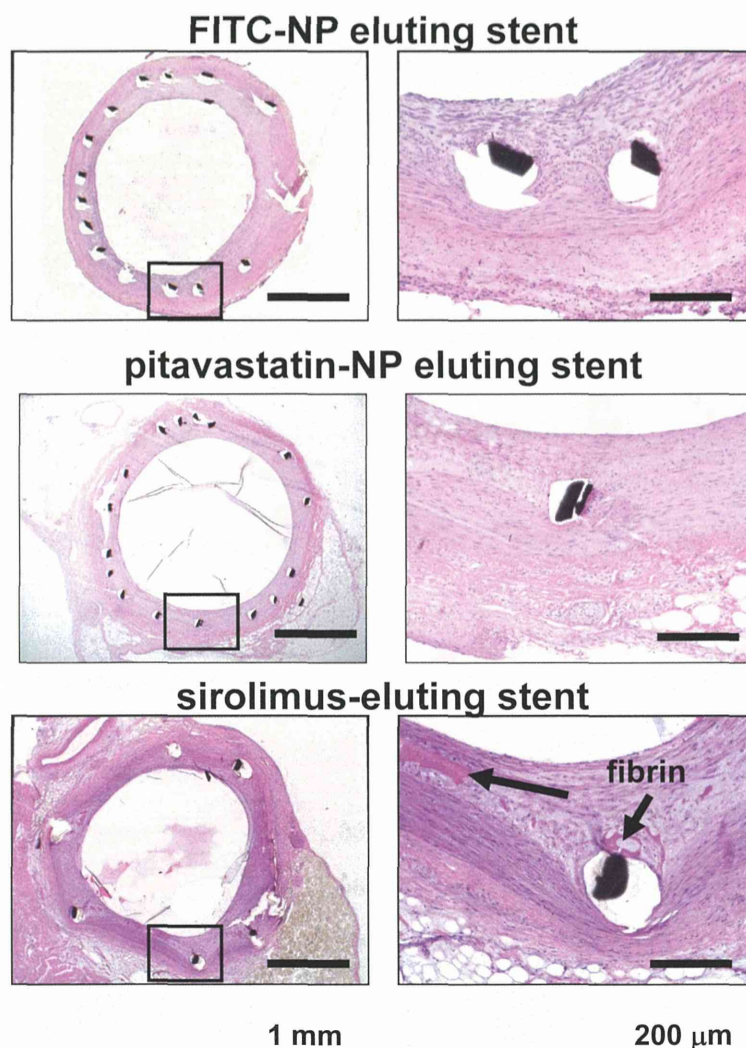


Fig. 6. Representative low- (left panels) and high-magnification (right panels) micrographs of coronary artery cross-sections stained with hematoxylin-eosin after four weeks from FITC-NP-eluting, pitavastatin-NP-eluting, and sirolimus-eluting stent groups.

sue factor expression (**Fig. 1** and **2**). A possible explanation for the discrepancy in the effect of VSMC proliferation between hydrophilic and lipophilic statins is that, under *in vitro* conditions, hydrophilic statins are hardly incorporated into vascular tissues or vascular smooth muscle cells while lipophilic statins are more widely taken up by vascular tissues and cells via passive diffusion. Pitavastatin normalized sirolimus-induced inhibition of eNOS activity in human endothelial cells (**Fig. 3**). In addition, pitavastatin-NP was as effective as non-nanoparticulated pitavastatin at an approximately 100-fold lower dose for inhibition of VSMC proliferation (**Fig. 4**). Collectively, these *in vitro* data suggest that the NP-mediated delivery of

pitavastatin may be more effective than pitavastatin alone in inhibiting VSMC proliferation and tissue factor expression and in promoting re-endothelialization.

We previously reported the central role of monocyte-mediated inflammation in the pathogenesis of in-stent neointima formation²⁸⁻³¹) and the formulation of polymeric gene-eluting stents or nuclear factor kappa-B decoy, inhibiting in-stent stenosis^{28, 32}); however, although advanced polymer technology was used, we were not able to formulate appropriate statin coating on metallic stents (authors' unpublished observation). An important finding of this study is that pitavastatin-NP-eluting stents attenuated in-stent stenosis (neointima formation) as effectively as sirolimus-eluting

Table 3. Re-endothelialization, injury score, inflammation score, and fibrin score 4 weeks after stenting

	BMS (n=10)	FITC-NP stent (n=12)	Pitavastatin -NP stent (n=12)	SES (n=12)	p value
Re-endothelialization score	2.70 ± 0.15	2.83 ± 0.11	2.83 ± 0.11	2.08 ± 0.43	NS
Injury score	1.31 ± 0.03	1.39 ± 0.07	1.36 ± 0.05	1.42 ± 0.11	NS
Inflammation score	1.65 ± 0.14	1.64 ± 0.07	1.08 ± 0.14*	2.38 ± 0.12**	p < 0.0001
Fibrin score	0.30 ± 0.15	0.58 ± 0.19	0.65 ± 0.18	2.00 ± 0.21**	p < 0.0001

Data are the mean ± SEM. * $p < 0.05$, ** $p < 0.01$ versus control bare metal stent by Kruskal-Wallis test followed with non-parametric Dunn's multiple comparison tests. NS: Not Significant.

The re-endothelialization score was defined as the extent of the circumference of the arterial lumen covered by endothelial cells and was scored from 1 to 3 (1=25%; 2=25% to 75%; 3=>75%).

The injury score was determined at each strut site, and mean values were calculated for each stented segment. In brief, a numeric value from 0 (no injury) to 3 (most injury) was assigned: 0=endothelial denudate, internal elastica lamina (IEL) intact; 1=IEL lacerated, media compressed, not lacerated; 2=IEL lacerated, media lacerated, external elastica lamina (EEL) compressed, not lacerated; and 3=media severely lacerated, EEL lacerated, adventitial may contain stent strut. The average injury score for each segment was calculated by dividing the sum of injury scores by the total number of struts in the examined section.

The inflammation score took into consideration the extent and density of the inflammatory infiltrate in each individual strut. With regard to the inflammation score for each individual strut, the grading is: 0=no inflammatory cells surrounding the strut; 1=light, non-circumferential inflammatory cell infiltrate surrounding the strut; 2=localized, moderate to dense cellular aggregate surrounding the strut non-circumferentially; and 3=circumferential dense inflammatory cell infiltration of the strut. The inflammation score for each cross section was calculated in the same manner as for the injury score (sum of the individual inflammatory scores, divided by the number of struts in the examined section).

The intimal fibrin content was graded as 0, no residual fibrin; 1, focal regions of residual fibrin involving any portion of the artery or moderate fibrin deposition adjacent to the strut involving <25% of the circumference of the artery; 2, moderate fibrin involving >25% of the circumference of the artery or heavy deposition involving <25% of the circumference of the artery; or 3, heavy fibrin deposition involving >25% of the circumference of the artery.

Table 4. Effects of intracoronary saline or Pitava-NP on histopathological morphometry and scoring 4 weeks after stenting

	saline (n=5)	Pitavastatin-NP 300 µg (n=6)	Pitavastatin-NP 3000 µg (n=6)	p value
Morphometry at stent sites				
Lumen area	2.88 ± 0.25	2.29 ± 1.01	2.72 ± 0.88	NS
Media area	0.95 ± 0.12	1.25 ± 0.32	0.92 ± 0.13	NS
Neointimal area	1.80 ± 0.14	2.30 ± 0.93	1.92 ± 0.88	NS
Scores at stent sites				
Injury score	1.00 ± 0.0	1.22 ± 0.13	1.04 ± 0.05	NS
Inflammation score	1.33 ± 0.0	1.47 ± 0.46	1.23 ± 0.08	NS
Fibrin score	0.75 ± 0.09	0.74 ± 0.27	0.39 ± 0.16*	p < 0.05
Endothelization score	2.00 ± 0.0	1.80 ± 0.27	1.98 ± 0.03	NS

Data are the mean ± SEM. * $p < 0.05$ versus control bare metal stent by Kruskal-Wallis test followed with non-parametric Dunn's multiple comparison tests. NS: not significant.

stents in a porcine coronary artery model. It is likely that local mechanisms are involved in the mechanism of the therapeutic effects of pitavastatin-NP eluting stents, because intracoronary administration of pitavastatin-NP at 300 µg (an equivalent dose to that coated on pitavastatin-NP-eluting stent) showed no effects. A prior study reported that oral administration of pitavastatin at 40 mg/body per day for five weeks inhibited in-stent stenosis in a porcine coronary artery model¹². The estimated dose of pitavastatin loaded on our NP-eluting stent was 20 ± 4 µg/stent, which is

much lower than the cumulative systemic dose used in a prior study (40 × 35 days = 1350 mg/body)¹². We measured the local tissue concentrations of pitavastatin with HPLC and found them to be under the limit of detection immediately after the deployment of the pitavastatin-NP-eluting stent; therefore, the local concentration of pitavastatin after deployment of the pitavastatin-NP-eluting stent is unclear, but is less than the limit of detection (2.5 ng/g protein or 1 ng/mL).

Delayed endothelial healing effects characterized

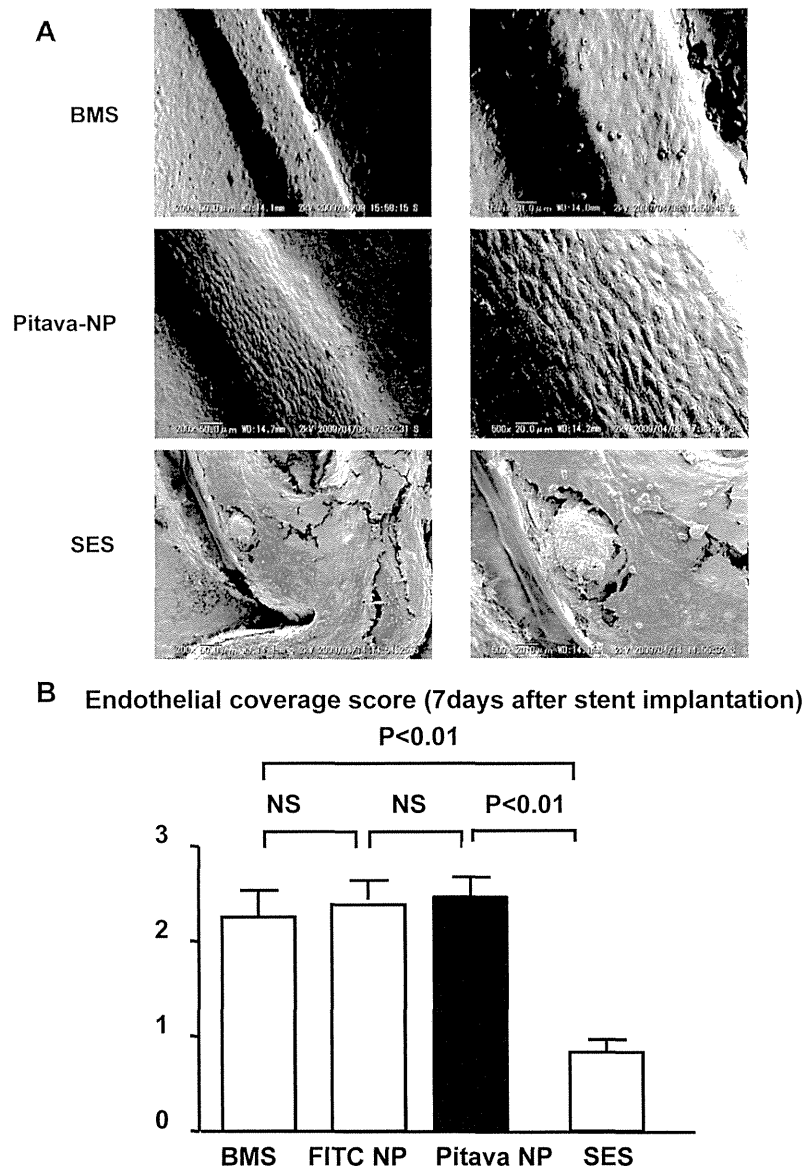


Fig. 7. Endothelial surface coverage analysis by scanning electron microscopy.

A, Representative micrographs of the endothelial surface by scanning electron microscopy one week after stent implantation. B, Endothelial coverage score one week after stent implantation in bare metal stent (BMS), FITC-NP-eluting stent (FITC-NP), pitavastatin-NP-eluting stent (Pitava-NP) stent, and sirolimus-eluting stent (SES) groups ($n = 3$ each).

by impaired re-endothelialization and persistence of fibrin and inflammation are an important histopathological feature in arteries exposed to currently marketed DESs in experimental animals^{33, 34} and in humans⁴⁻⁶. These delayed endothelial healing effects are presumed to result from the effects of drugs coated on DESs (see Introduction). Using human pathological data from autopsy patients in whom death occurred >30 days after drug-eluting stent placement, Finn *et al.*⁶ dem-

onstrated that endothelialization of the stent was the best predictor of late in-stent thrombosis. Heterogeneity of healing is a common finding in cases of late drug-eluting stent thrombosis. In this study, we confirmed the delayed endothelial healing effects of sirolimus-eluting stents in porcine coronary arteries (**Fig. 5, 6, and 7**) reported by Virmani's group⁵; however, we found that pitavastatin-NP-eluting stents had no such delayed endothelial healing effects in porcine coronary

arteries *in vivo*. The opposing effects of pitavastatin-NP-eluting stents and sirolimus-eluting stents might be explained by our *in vitro* study (Fig. 1 and 2). Collectively, these data on anti-endothelial healing properties suggest that pitavastatin-NP-eluting stents may have an advantage over currently marketed polymeric DES devices. Future studies are needed to prove this point.

A major limitation of this study is that this study was performed in normal pigs without pre-existing atherosclerotic coronary lesions, although this porcine coronary artery model is regarded as an appropriate and standard preclinical study model³⁵). A long-term efficacy study is also needed.

In conclusion, pitavastatin-NP-eluting stents not only attenuated in-stent stenosis as effectively as polymer-coated sirolimus-eluting stents but also elicited endothelial healing effects in a porcine coronary artery model. Delayed endothelial healing is a common feature at atherosclerotic arterial sites deployed with currently marketed DESs, which may lead to an increased risk of late stent thrombosis. Our present technology can be one approach to overcome the adverse effects of current DESs and may provide the optimal anti-healing combination: the inhibition of VSMC proliferation to decrease restenosis and the promotion of re-endothelialization to protect from late stent thrombosis. This NP-eluting stent system may be developed as an innovative platform for the future treatment of atherosclerotic vascular disease.

Acknowledgments

Funding Sources: This study was supported by Grants-in-Aid for Scientific Research (19390216, 19650134) from the Ministry of Education, Science, and Culture, Tokyo, Japan, by Health Science Research Grants (Research on Translational Research and Nanomedicine) from the Ministry of Health Labor and Welfare, Tokyo, Japan, and by a Special Grant from Terumo Life Science Foundation, Tokyo, Japan.

Conflict of Interest

Dr. Egashira holds a patent on the results reported in the present study. The remaining authors report no conflicts.

References

- 1) Laskey WK, Yancy CW, Maisel WH: Thrombosis in coronary drug-eluting stents: Report from the meeting of the circulatory system medical devices advisory panel of the food and drug administration center for devices and radiologic health, december 7-8, 2006. *Circulation*, 2007; 115: 2352-2357
- 2) Serruys PW, Kutryk MJ, Ong AT: Coronary-artery stents. *N Engl J Med*, 2006; 354: 483-495
- 3) Shuchman M: Trading restenosis for thrombosis? New questions about drug-eluting stents. *N Engl J Med*, 2006; 355: 1949-1952
- 4) Luscher TF, Steffel J, Eberli FR, Joner M, Nakazawa G, Tanner FC, Virmani R: Drug-eluting stent and coronary thrombosis: Biological mechanisms and clinical implications. *Circulation*, 2007; 115: 1051-1058
- 5) Finn AV, Nakazawa G, Joner M, Kolodgie FD, Mont EK, Gold HK, Virmani R: Vascular responses to drug eluting stents. Importance of delayed healing. *Arterioscler Thromb Vasc Biol*, 2007; 27: 1500-1510
- 6) Finn AV, Joner M, Nakazawa G, Kolodgie F, Newell J, John MC, Gold HK, Virmani R: Pathological correlates of late drug-eluting stent thrombosis: Strut coverage as a marker of endothelialization. *Circulation*, 2007; 115: 2435-2441
- 7) Joner M, Nakazawa G, Finn AV, Quee SC, Coleman L, Acampado E, Wilson PS, Skorija K, Cheng Q, Xu X, Gold HK, Kolodgie FD, Virmani R: Endothelial cell recovery between comparator polymer-based drug-eluting stents. *J Am Coll Cardiol*, 2008; 52: 333-342
- 8) Takemoto M, Liao JK: Pleiotropic effects of 3-hydroxy-3-methylglutaryl coenzyme a reductase inhibitors. *Arterioscler Thromb Vasc Biol*, 2001; 21: 1712-1719
- 9) Eto M, Kozai T, Cosentino F, Joch H, Luscher TF: Statin prevents tissue factor expression in human endothelial cells: Role of rho/rho-kinase and akt pathways. *Circulation*, 2002; 105: 1756-1759
- 10) Thyberg J: Re-endothelialization via bone marrow-derived progenitor cells: Still another target of statins in vascular disease. *Arterioscler Thromb Vasc Biol*, 2002; 22: 1509-1511
- 11) Werner N, Priller J, Laufs U, Endres M, Bohm M, Dirnagl U, Nickenig G: Bone marrow-derived progenitor cells modulate vascular reendothelialization and neointimal formation: Effect of 3-hydroxy-3-methylglutaryl coenzyme a reductase inhibition. *Arterioscler Thromb Vasc Biol*, 2002; 22: 1567-1572
- 12) Yokoyama T, Miyauchi K, Kurata T, Satoh H, Daida H: Inhibitory efficacy of pitavastatin on the early inflammatory response and neointimal thickening in a porcine coronary after stenting. *Atherosclerosis*, 2004; 174: 253-259
- 13) Indolfi C, Cioppa A, Stabile E, Di Lorenzo E, Esposito G, Pisani A, Leccia A, Cavuto L, Stingone AM, Chieffo A, Capozzolo C, Chiariello M: Effects of hydroxymethylglutaryl coenzyme a reductase inhibitor simvastatin on smooth muscle cell proliferation in vitro and neointimal formation in vivo after vascular injury. *J Am Coll Cardiol*, 2000; 35: 214-221
- 14) Scheller B, Schmitt A, Bohm M, Nickenig G: Atorvastatin stent coating does not reduce neointimal proliferation after coronary stenting. *Zeitschrift fur Kardiologie*, 2003; 92: 1025-1028
- 15) Miyauchi K, Kasai T, Yokoyama T, Aihara K, Kurata T, Kajimoto K, Okazaki S, Ishiyama H, Daida H: Effectiveness of statin-eluting stent on early inflammatory response

- and neointimal thickness in a porcine coronary model. *Circ J*, 2008; 72: 832-838
- 16) Serruys PW, Foley DP, Jackson G, Bonnier H, Macaya C, Vrolix M, Branzi A, Shepherd J, Suryapranata H, de Feyter PJ, Melkert R, van Es GA, Pfister PJ: A randomized placebo-controlled trial of fluvastatin for prevention of restenosis after successful coronary balloon angioplasty; final results of the fluvastatin angiographic restenosis (flare) trial. *Eur Heart J*, 1999; 20: 58-69
 - 17) Bertrand ME, McFadden EP, Fruchart JC, Van Belle E, Commeau P, Grollier G, Bassand JP, Machecourt J, Cassagnes J, Mossard JM, Vacheron A, Castaigne A, Danchin N, Lablanche JM: Effect of pravastatin on angiographic restenosis after coronary balloon angioplasty. The predict trial investigators. Prevention of restenosis by elisor after transluminal coronary angioplasty. *J Am Coll Cardiol*, 1997; 30: 863-869
 - 18) Weintraub WS, Boccuzzi SJ, Klein JL, Kosinski AS, King SB, 3rd, Ivanhoe R, Cedarholm JC, Stillabower ME, Talley JD, DeMaio SJ, et al: Lack of effect of lovastatin on restenosis after coronary angioplasty. Lovastatin restenosis trial study group. *N Engl J Med*, 1994; 331: 1331-1337
 - 19) Onaka H, Hirota Y, Kita Y, Tsuji R, Ishii K, Ishimura T, Kawamura K: The effect of pravastatin on prevention of restenosis after successful percutaneous transluminal coronary angioplasty. *Jpn Circ J*, 1994; 58: 100-106
 - 20) Bae JH, Bassenge E, Kim KY, Synn YC, Park KR, Schwemmer M: Effects of low-dose atorvastatin on vascular responses in patients undergoing percutaneous coronary intervention with stenting. *J Cardiovasc Pharmacol Ther*, 2004; 9: 185-192
 - 21) Petronio AS, Amoroso G, Limbruno U, Papini B, De Carlo M, Micheli A, Ciabatti N, Mariani M: Simvastatin does not inhibit intimal hyperplasia and restenosis but promotes plaque regression in normocholesterolemic patients undergoing coronary stenting: A randomized study with intravascular ultrasound. *Am Heart J*, 2005; 149: 520-526
 - 22) Nakano K, Egashira K, Masuda S, Funakoshi K, Zhao G, Kimura S, Matoba T, Sueishi K, Endo Y, Kawashima Y, Hara K, Tsujimoto H, Tominaga R, Sunagawa K: Formulation of nanoparticle-eluting stents by a cationic electrodeposition coating technology efficient nano-drug delivery via bioabsorbable polymeric nanoparticle-eluting stents in porcine coronary arteries. *JACC Cardiovasc Interv*, 2009; 2: 277-283
 - 23) Kimura S, Egashira K, Nakano K, Iwata E, Miyagawa M, Tsujimoto H, Hara K, Kawashima Y, Tominaga R, Sunagawa K: Local delivery of imatinib mesylate (sti571)-incorporated nanoparticle ex vivo suppresses vein graft neointima formation. *Circulation*, 2008; 118: S65-70
 - 24) Masuda S, Nakano K, Funakoshi K, Zhao G, Meng W, Kimura S, Matoba T, Miyagawa M, Iwata E, Sunagawa K, Egashira K: Imatinib mesylate-incorporated nanoparticle-eluting stent attenuates in-stent neointimal formation in porcine coronary arteries. *J Atheroscler Thromb*, 2011; 18: 1043-1053
 - 25) Aoki T, Nishimura H, Nakagawa S, Kojima J, Suzuki H, Tamaki T, Wada Y, Yokoo N, Sato F, Kimata H, Kitahara M, Toyoda K, Sakashita M, Saito Y: Pharmacological profile of a novel synthetic inhibitor of 3-hydroxy-3-methylglutaryl-coenzyme a reductase. *Arzneimittel-Forschung*, 1997; 47: 904-909
 - 26) Ohtani K, Usui M, Nakano K, Kohjimoto Y, Kitajima S, Hirouchi Y, Li XH, Kitamoto S, Takeshita A, Egashira K: Antimonocyte chemoattractant protein-1 gene therapy reduces experimental in-stent restenosis in hypercholesterolemic rabbits and monkeys. *Gene Ther*, 2004; 11: 1273-1282
 - 27) Camici GG, Steffel J, Akhmedov A, Schafer N, Baldinger J, Schulz U, Shojaati K, Matter CM, Yang Z, Luscher TF, Tanner FC: Dimethyl sulfoxide inhibits tissue factor expression, thrombus formation, and vascular smooth muscle cell activation: A potential treatment strategy for drug-eluting stents. *Circulation*, 2006; 114: 1512-1521
 - 28) Egashira K, Nakano K, Ohtani K, Funakoshi K, Zhao G, Ihara Y, Koga J, Kimura S, Tominaga R, Sunagawa K: Local delivery of anti-monocyte chemoattractant protein-1 by gene-eluting stents attenuates in-stent stenosis in rabbits and monkeys. *Arterioscler Thromb Vasc Biol*, 2007; 27: 2563-2568
 - 29) Usui M, Egashira K, Ohtani K, Kataoka C, Ishibashi M, Hiasa K, Katoh M, Zhao Q, Kitamoto S, Takeshita A: Anti-monocyte chemoattractant protein-1 gene therapy inhibits restenotic changes (neointimal hyperplasia) after balloon injury in rats and monkeys. *FASEB J*, 2002; 16: 1838-1840
 - 30) Egashira K, Zhao Q, Kataoka C, Ohtani K, Usui M, Charo IF, Nishida K, Inoue S, Katoh M, Ichiki T, Takeshita A: Importance of monocyte chemoattractant protein-1 pathway in neointimal hyperplasia after periarterial injury in mice and monkeys. *Circ Res*, 2002; 90: 1167-1172
 - 31) Egashira K: Molecular mechanisms mediating inflammation in vascular disease: Special reference to monocyte chemoattractant protein-1. *Hypertension*, 2003; 41: 834-841
 - 32) Ohtani K, Egashira K, Nakano K, Zhao G, Funakoshi K, Ihara Y, Kimura S, Tominaga R, Morishita R, Sunagawa K: Stent-based local delivery of nuclear factor-kappaB decoy attenuates in-stent restenosis in hypercholesterolemic rabbits. *Circulation*, 2006; 114: 2773-2779
 - 33) van der Giessen WJ, Lincoff AM, Schwartz RS, van Beusekom HM, Serruys PW, Holmes DR Jr, Ellis SG, Topol EJ: Marked inflammatory sequelae to implantation of biodegradable and nonbiodegradable polymers in porcine coronary arteries. *Circulation*, 1996; 94: 1690-1697
 - 34) Lincoff AM, Furst JG, Ellis SG, Tuch RJ, Topol EJ: Sustained local delivery of dexamethasone by a novel intravascular eluting stent to prevent restenosis in the porcine coronary injury model. *J Am Coll Cardiol*, 1997; 29: 808-816
 - 35) Schwartz RS, Edelman ER, Carter A, Chronos N, Rogers C, Robinson KA, Waksman R, Weinberger J, Wilensky RL, Jensen DN, Zuckerman BD, Virmani R: Drug-eluting stents in preclinical studies: Recommended evaluation from a consensus group. *Circulation*, 2002; 106: 1867-1873

Nanoparticle-Mediated Delivery of Pitavastatin Inhibits Atherosclerotic Plaque Destabilization/Rupture in Mice by Regulating the Recruitment of Inflammatory Monocytes

Shunsuke Katsuki, MD; Tetsuya Matoba, MD, PhD; Soichi Nakashiro, MD; Kei Sato, PhD; Jun-ichiro Koga, MD, PhD; Kaku Nakano, PhD; Yasuhiro Nakano, MD; Shizuka Egusa, PhD; Kenji Sunagawa, MD, PhD; Kensuke Egashira, MD, PhD

Background—Preventing atherosclerotic plaque destabilization and rupture is the most reasonable therapeutic strategy for acute myocardial infarction. Therefore, we tested the hypotheses that (1) inflammatory monocytes play a causative role in plaque destabilization and rupture and (2) the nanoparticle-mediated delivery of pitavastatin into circulating inflammatory monocytes inhibits plaque destabilization and rupture.

Methods and Results—We used a model of plaque destabilization and rupture in the brachiocephalic arteries of apolipoprotein E-deficient (ApoE^{-/-}) mice fed a high-fat diet and infused with angiotensin II. The adoptive transfer of CCR2^{+/+}Ly-6C^{high} inflammatory macrophages, but not CCR2^{-/-} leukocytes, accelerated plaque destabilization associated with increased serum monocyte chemoattractant protein-1 (MCP-1), monocyte-colony stimulating factor, and matrix metalloproteinase-9. We prepared poly(lactic-co-glycolic) acid nanoparticles that were incorporated by Ly-6G-CD11b⁺ monocytes and delivered into atherosclerotic plaques after intravenous administration. Intravenous treatment with pitavastatin-incorporated nanoparticles, but not with control nanoparticles or pitavastatin alone, inhibited plaque destabilization and rupture associated with decreased monocyte infiltration and gelatinase activity in the plaque. Pitavastatin-incorporated nanoparticles inhibited MCP-1-induced monocyte chemotaxis and the secretion of MCP-1 and matrix metalloproteinase-9 from cultured macrophages. Furthermore, the nanoparticle-mediated anti-MCP-1 gene therapy reduced the incidence of plaque destabilization and rupture.

Conclusions—The recruitment of inflammatory monocytes is critical in the pathogenesis of plaque destabilization and rupture, and nanoparticle-mediated pitavastatin delivery is a promising therapeutic strategy to inhibit plaque destabilization and rupture by regulating MCP-1/CCR2-dependent monocyte recruitment in this model. (*Circulation*. 2014;129:896-906.)

Key Words: monocytes ■ myocardial infarction ■ nanoparticles ■ plaque ■ statins, HMG-CoA

Coronary heart disease is the leading cause of death worldwide, and at least 7 million patients die of this disease each year (386 324 people in the United States alone).¹ Acute myocardial infarction (AMI) is the most severe type of coronary heart disease and the most frequent cause of heart failure, and it impairs the quality of life and inflates medical costs. Timely and successful revascularization therapy for AMI reduces short-term mortality, and current standard medical therapy with angiotensin-converting enzyme inhibitors and β -blockers ameliorates the development of post-myocardial infarction heart failure. However, these recent advances in therapeutic intervention for AMI are associated with an increased prevalence of heart failure with high long-term mortality, which remains a serious concern.² In the United States, 5.1 million people experienced heart failure in 2010, and 274 601 people

died of heart failure in 2009.¹ Therefore, there is an urgent need for preventive treatment to avoid plaque destabilization and rupture, which directly cause AMI.

Clinical Perspective on p 906

Rupture-prone unstable atherosclerotic plaques feature monocyte/macrophage infiltration, lipid core formation, and fibrous cap thinning by matrix metalloproteinases (MMPs).³ Recent reports suggest that monocytes are functionally polarized into at least 2 major subsets: Inflammatory monocytes (CD14⁺CD16⁻ in humans and Ly-6C^{high}CCR2⁺CX3CR1^{low} in mice) and anti-inflammatory monocytes (CD14⁺CD16⁺ in humans and Ly-6C^{low}CCR2⁻CX3CR1^{high} in mice).⁴ Inflammatory monocytes are found in the peripheral blood of patients with AMI,⁵

Received April 2, 2013; accepted November 15, 2013.

From the Department of Cardiovascular Medicine (S.K., T.M., S.N., J.K., Y.N., S.E., K. Sunagawa) and Department of Cardiovascular Research, Development, and Translational Medicine (K. Sato, K.N., K.E.), Kyushu University Graduate School of Medical Sciences, Fukuoka, Japan.

The online-only Data Supplement is available with this article at <http://circ.ahajournals.org/lookup/suppl/doi:10.1161/CIRCULATIONAHA.113.002870/-/DC1>.

Correspondence to Kensuke Egashira, MD, PhD, FAHA, Department of Cardiovascular Research, Development, and Translational Medicine, Kyushu University Graduate School of Medical Sciences, 3-1-1 Maidashi, Higashi-ku, Fukuoka 812-8582, Japan. E-mail egashira@cardiol.med.kyushu-u.ac.jp

© 2013 American Heart Association, Inc.

Circulation is available at <http://circ.ahajournals.org>

DOI: 10.1161/CIRCULATIONAHA.113.002870

which suggests that they have a pathological role in plaque destabilization; however, substantial proof for a causative role of inflammatory monocytes in the pathogenesis of plaque destabilization and rupture is lacking.

HMG-CoA reductase inhibitors (statins) lower serum cholesterol levels and reduce cardiovascular events and mortality by 32% to 37% in primary prevention trials^{6,7} and 24% to 30% in secondary prevention trials.^{8,9} Data from clinical trials indicate that although the intensive use of statins reduces serum C-reactive protein levels and cardiovascular risk and attenuates the progression of coronary artery plaque,^{10–13} the risk reduction caused by on-label doses of statins remains insufficient to suppress AMI.¹⁰ In animals, plaque-stabilizing effects have been observed after high doses of statins.^{14–18} Statins exert multiple vasculoprotective effects on endothelial cells, vascular smooth muscle cells, and monocytes.^{19–21} Thus, we hypothesized that the controlled delivery of statins to inflammatory monocytes and atherosclerotic plaques might optimize the plaque-stabilizing effects of statins.

Recently, we developed a novel nanoparticle-mediated drug-delivery system (DDS) that is formulated from bioabsorbable poly(lactic-co-glycolic) acid (PLGA) polymer, and we reported that nanoparticles were taken up by a variety of cells, such as monocytes, vascular smooth muscle cells, and endothelial cells. In addition, the nanoparticle-mediated DDS showed a significant enhancement in the therapeutic effects on ischemia-induced neovascularization^{22,23} and pulmonary arterial hypertension²⁴ in animal models compared with conventional administration. Nanoparticles are rapidly taken up by circulating monocytes and the mononuclear phagocytic system after intravenous administration,²⁵ and nano-sized contrast agents accumulate in atherosclerotic plaques.²⁶ To the best of our knowledge, no prior studies have addressed whether polymeric nanoparticles accumulate in unstable atherosclerotic plaques after intravenous administration or whether the nanoparticle-mediated delivery of pitavastatin has therapeutic effects on plaque destabilization and rupture *in vivo*. Therefore, we tested the hypotheses that (1) inflammatory monocytes play a causative role in plaque destabilization and rupture and (2) the nanoparticle-mediated delivery of pitavastatin inhibits plaque destabilization and rupture by targeting inflammatory monocytes.

Methods

Experimental Animals

Male apolipoprotein E-deficient (ApoE^{-/-}) mice on the C57BL/6J genetic background were purchased from Jackson Laboratory (Bar Harbor, ME). ApoE^{-/-}CCR2^{-/-} and ApoE^{-/-}CCR2^{+/+} mice with the same genetic background (C57BL/6J and 129/svjae hybrids) were used.²⁷ Animals were maintained on a 12-hour light-dark cycle with free access to normal rodent chow and water.

Diet Preparation

A high-fat diet that contained 21% fat from lard and was supplemented with 0.15% (wt/wt) pure cholesterol (Oriental Yeast, Tokyo, Japan) was prepared according to the formula recommended by the American Institute of Nutrition. Additional details can be found in the online-only Data Supplement.

Experimental Protocol

The study protocol was reviewed and approved by the Committee on the Ethics of Animal Experiments, Kyushu University Graduate School of Medical Sciences. The 4 sets of animal experiments are depicted in a schematic in Figure I in the online-only Data Supplement. Brachiocephalic arteries were isolated with the aortic arches. Isolated samples were fixed in 3.7% formaldehyde for histological and immunohistochemical analyses or were snap-frozen in liquid nitrogen and stored at -80°C for biochemical analysis. Additional details for each experimental protocol can be found in the online-only Data Supplement.

Histopathology and Immunohistochemistry

Histopathological and immunohistochemical evaluations were performed to quantify atherosclerosis and examine both plaque morphology and the mechanism of plaque destabilization and rupture. Atherosclerotic plaques were stained with oil red O, and cross sections of the brachiocephalic arteries and aortic root were stained with elastica van Gieson, antimacrophage surface glycoprotein Mac3, and monocyte chemoattractant protein-1 (MCP-1). Additional details are provided in the online-only Data Supplement.

Flow Cytometry

Leukocytes from peripheral blood and the spleen and peritoneal cells were obtained from mice and analyzed with a FACSCalibur cytometer (Becton-Dickinson Biosciences, San Jose, CA). Additional details can be found in the online-only Data Supplement.

Preparation of PLGA Nanoparticles

PLGA nanoparticles encapsulated with FITC (FITC-NP), pitavastatin (pitavastatin-NP) and 7ND plasmid (7ND-NP) were prepared by use of an emulsion solvent diffusion method, as reported previously.^{22–24} Additional details can be found in the online-only Data Supplement.

In Vivo Kinetics of the Nanoparticles

Excised aortas from the atherosclerotic mice were intravenously injected with or without FITC-NP and were evaluated by stereoscopic and fluorescence microscopy. Sections of the brachiocephalic artery were evaluated by fluorescence microscopy or were stained with hematoxylin and eosin. Additional details can be found in the online-only Data Supplement.

In Situ Zymography

Gelatinase (MMP-2/gelatinase-A and MMP-9/gelatinase-B) activity was measured in unfixed frozen sections with quenched fluorescein-labeled gelatinase substrate (DQ gelatin; Invitrogen, Eugene, OR).²⁸ Additional details can be found in the online-only Data Supplement.

Gelatin Zymography

The lipopolysaccharide-induced gelatinase activity of RAW264.7 cells was measured with a gelatin Zymo electrophoresis kit (Primary Cell, Hokkaido, Japan) according to the manufacturer's directions. Additional details can be found in the online-only Data Supplement.

Real-Time Quantitative Reverse-Transcription Polymerase Chain Reaction

Real-time polymerase chain reaction amplification was performed with mouse cDNA with the use of the ABI PRISM 7000 sequence detection system (Applied Biosystems/Life Technologies, Carlsbad, CA), as described previously.²⁹ The polymerase chain reaction primers and TaqMan probes we used can be found in the online-only Data Supplement.